

***HST Imaging of  
Proto-Planetary and  
Very Young Planetary Nebulae  
Towards a New Understanding  
of their Formation***

**Raghvendra Sahai**

**Jet Propulsion Laboratory**

**California Institute of Technology**

# ***Mass Loss during Late Stellar Evolution***

- **Spherically Symmetric during AGB**
  - heavy, continuous mass loss produces dense, dusty, filled envelopes (CSEs)  
(e.g. Neri et al 1992, Sahai & Bieging 1992)
- **Drastic Changes in Geometry post-AGB**
  - bright rims, shell-like structures
  - variety of aspherical morphologies  
(e.g. elliptical or bipolar) (e.g. Schwarz, Corradi & Melnick 1992)

## ***Question***

- **What produces the change in mass loss geometry at the end of the AGB?**

## ***Pre-HST Paradigm***

- **(Generalised) Interacting Stellar Winds Model**
  - **Fast ( $>1000$  km/s) ionised stellar wind from post-AGB star interacts with AGB slow wind**
  - **AGB wind is equatorially dense**

**RESULT:**    axi-symmetric PN shell, shape depends  
                  on polar-equatorial density contrast

(Kwok, Purton & Fitzgerald 1978, Kwok 1982, Balick 1987)

Hydrodynamic Models    :Frank, Mellema, Icke, Balick etc; see review by Frank 2000)

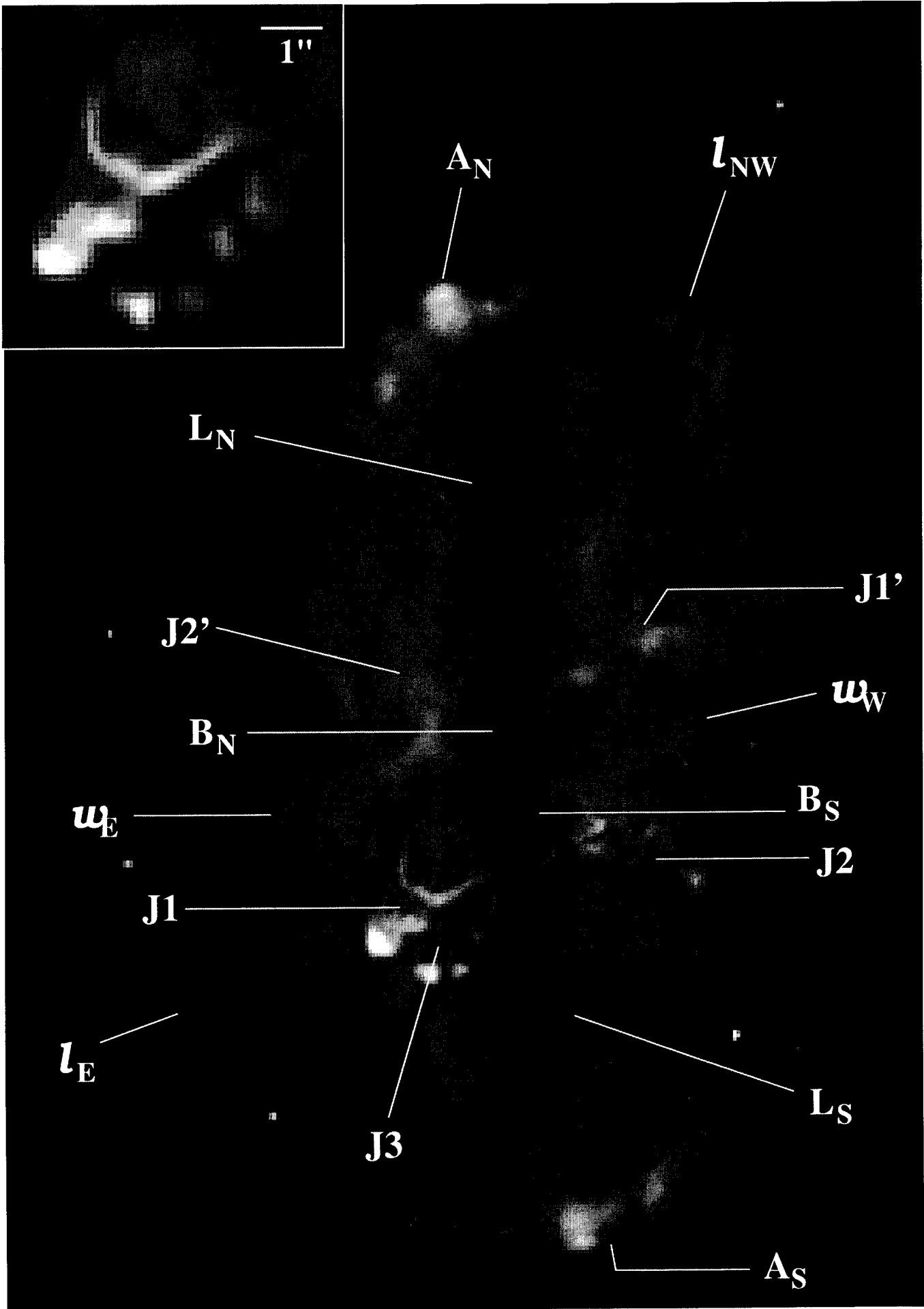
# ***Problems with GISW Model***

- **Nature/ Origin of Asymmetry in AGB CSE not known**
- **Non-Axisymmetric Morphologies in some PNe**
  - point-symmetric structures** (e.g. Corradi & Schwarz 1995)
  - jets, ansae, FLIERs** (e.g. Schwarz 1990, Balick et al. 1998)
  - quadrupolar structures** (e.g. Manchado et al 1996)
- **Fast (~100 km/s) bipolar outflows in a few PPNe & late AGB stars**  
(e.g. see review by Alcolea et al 2000)

Table 1. Summary of the results from the IRAM 30 m observations for sources showing high velocity molecular emission. Figures are corrected for distance, opacity, and axial inclination.  $V_{\text{exp}}$  is the maximum expansion velocity measured in CO;  $M_{\text{CE}}$  is the total mass of the molecular envelope;  $P_{\text{axial}}$  is the linear momentum along the axial directions;  $\text{Age}_{L_*}$  is the time required for the photon pressure to account for the axial momentum, i.e.  $P_{\text{axial}}/(L_*/c)$ ;  $\text{Age}_{\text{kin}}$  is the kinetic age of the high velocity outflow when measured

Object name	$V_{\text{exp}}$ ( $\text{km s}^{-1}$ )	$M_{\text{CE}}$ ( $M_{\odot}$ )	$P_{\text{axial}}$ ( $\text{gr cm/s}$ )	$L_*$ ( $L_{\odot}$ )	$\text{Age}_{L_*}$ (yr)	$\text{Age}_{\text{kin}}$ (yr)
OH 231.8	375	1.0	$3 \cdot 10^{39}$	$10^4$	70 000	750
M 1-92	70	0.9	$3 \cdot 10^{39}$	$10^4$	70 000	950
M 2-56	90	.07	$7 \cdot 10^{38}$	$10^4$	30 000	1 800
Frosty Leo	235	.09	$9 \cdot 10^{38}$	$3 \cdot 10^3$	80 000	<del>~ 1 000</del>
He 3-1475	70	.07	$3 \cdot 10^{38}$	$10^3$	50 000	<del>~ 800</del>
IRC +10420	50	2.0	$10^{40}$	$7 \cdot 10^5$	5 000	few 100
CRL 2688	190	0.7	$5 \cdot 10^{39}$	$4 \cdot 10^4$	30 000	
CRL 618	240	0.6	$2 \cdot 10^{39}$	$3 \cdot 10^4$	10 000	
IRAS 1743	28	0.6	$2 \cdot 10^{39}$	$6 \cdot 10^4$	6 000	
IRAS 1911	44	.04	$2 \cdot 10^{39}$	$3 \cdot 10^4$	20 000	
IRAS 1950	55	.03	$8 \cdot 10^{37}$	$2 \cdot 10^3$	10 000	
IRAS 2227	25	.07	$10^{38}$	$8 \cdot 10^3$	4 000	

(from Alcolea et al 2000)



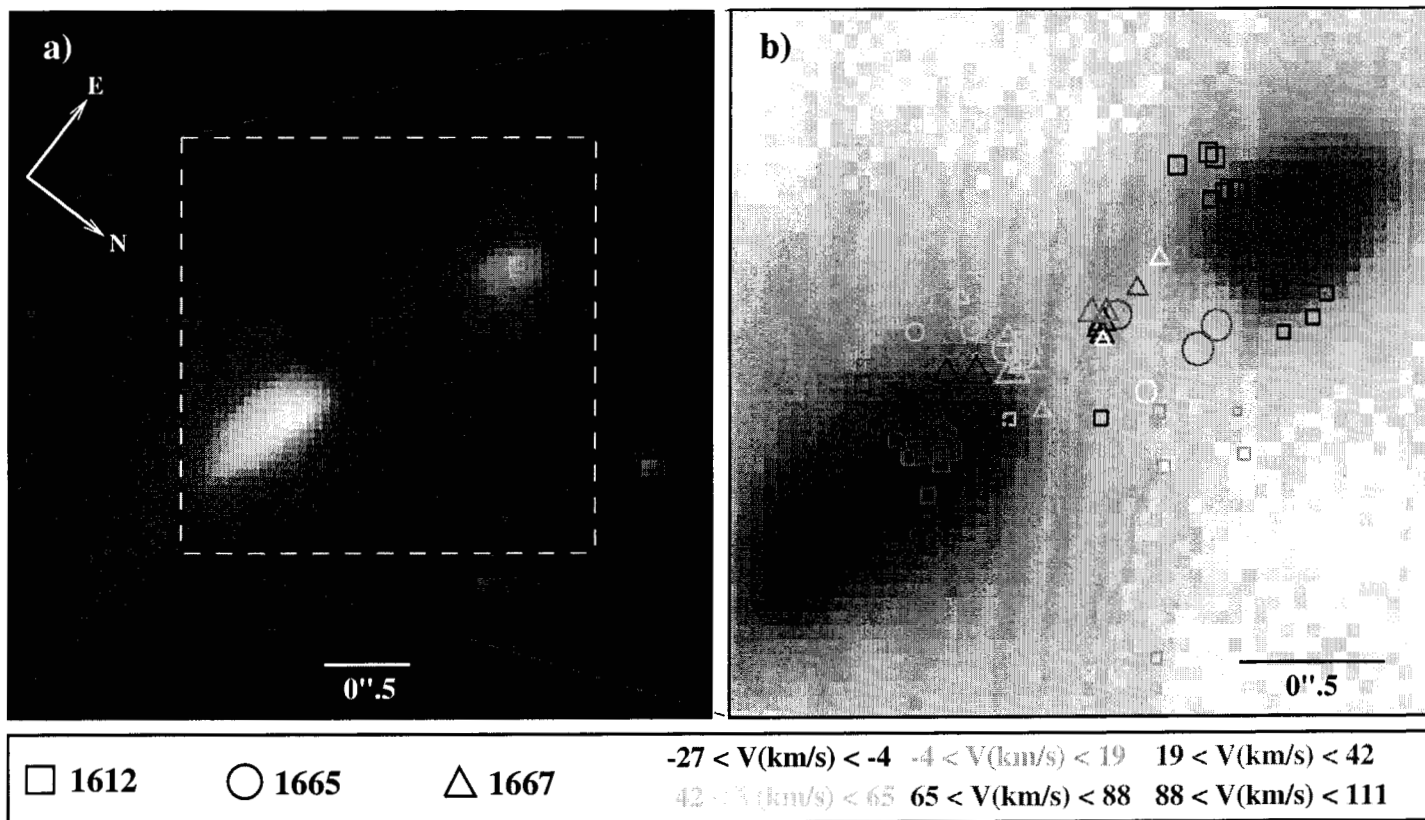


FIGURE 1

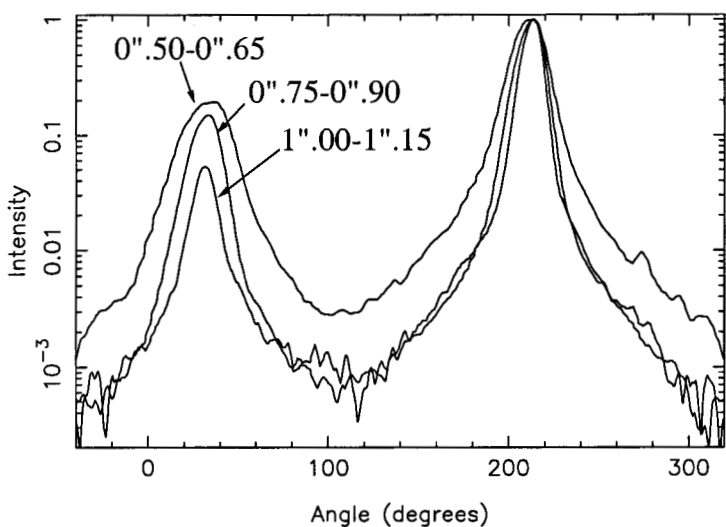


FIGURE 2

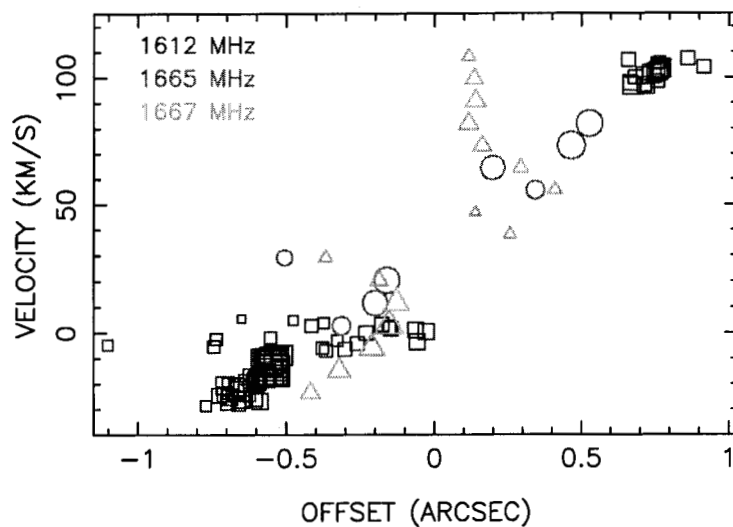
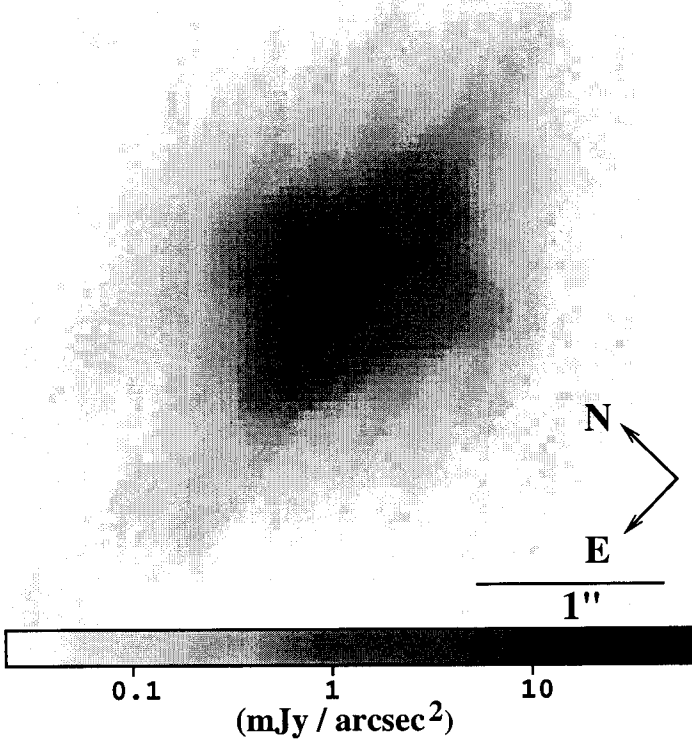
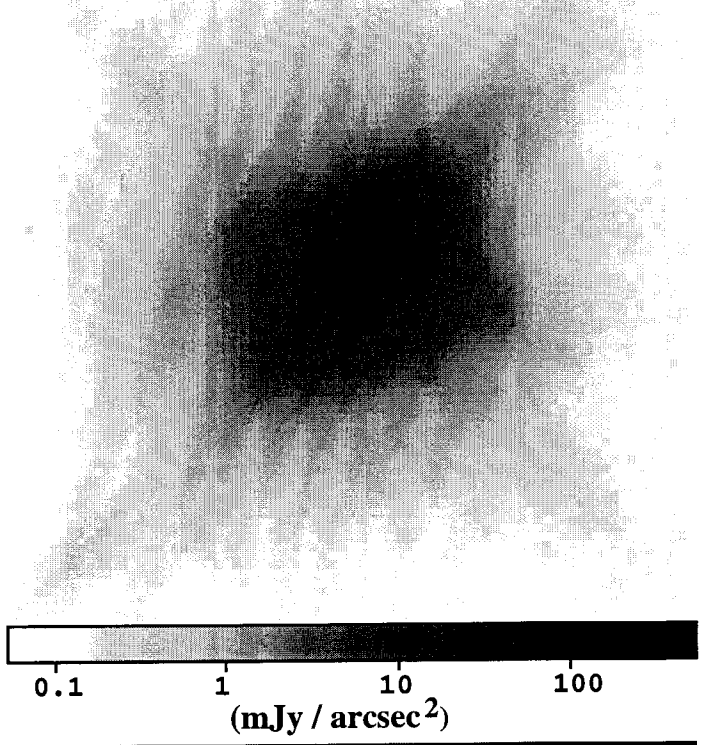


FIGURE 3

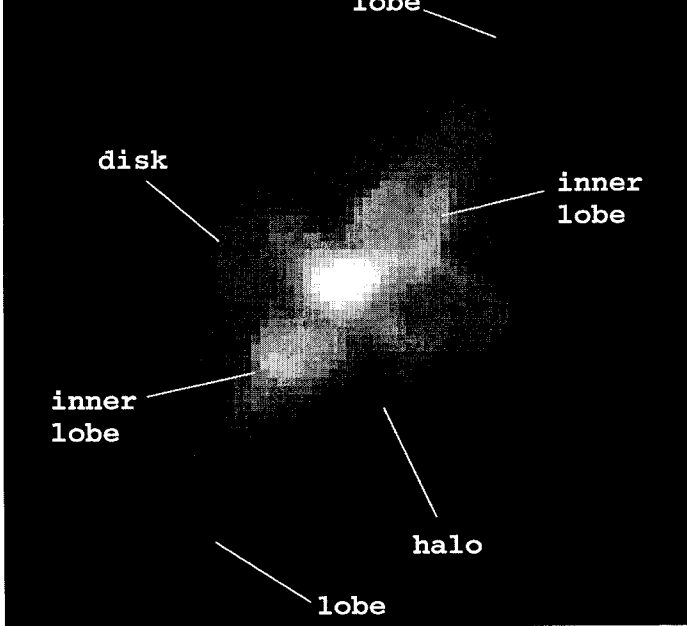
(a) F555W



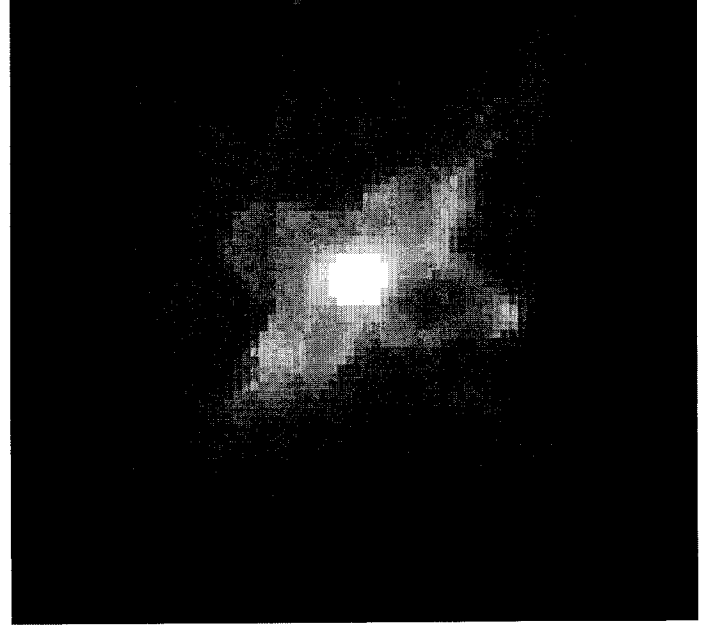
(b) F814W

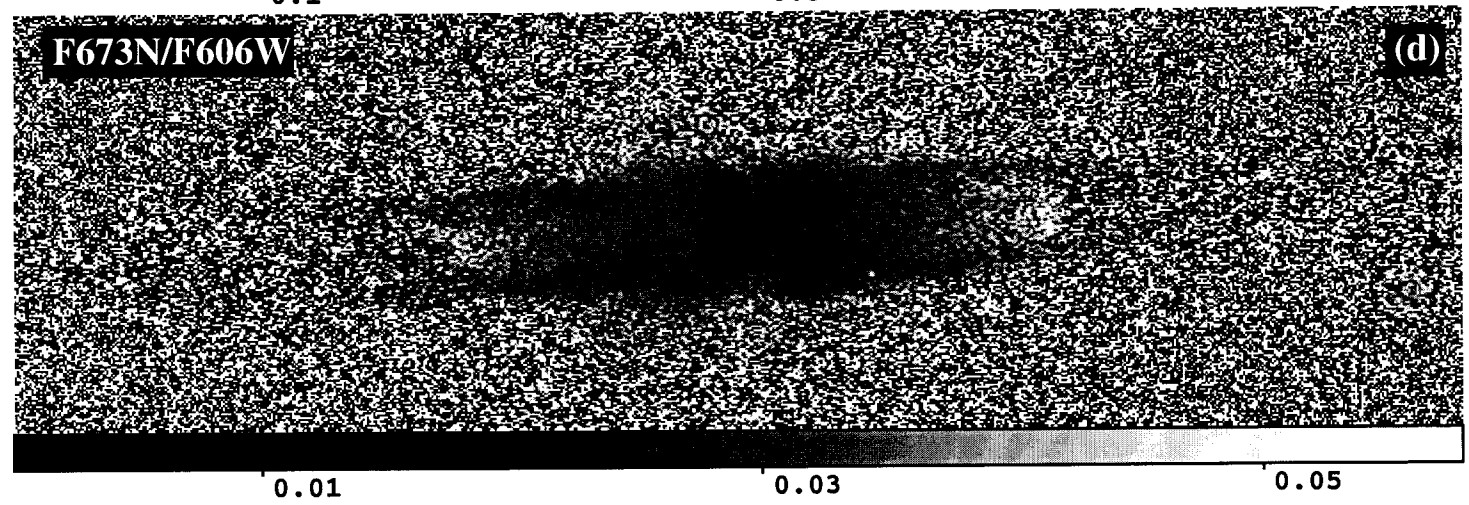
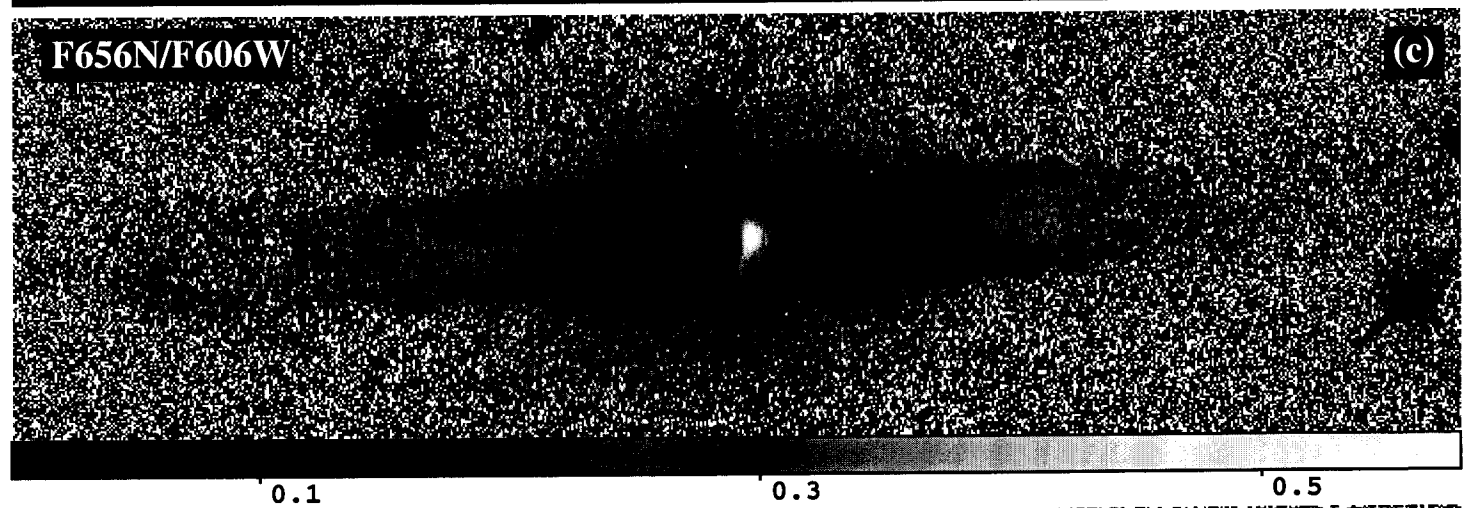
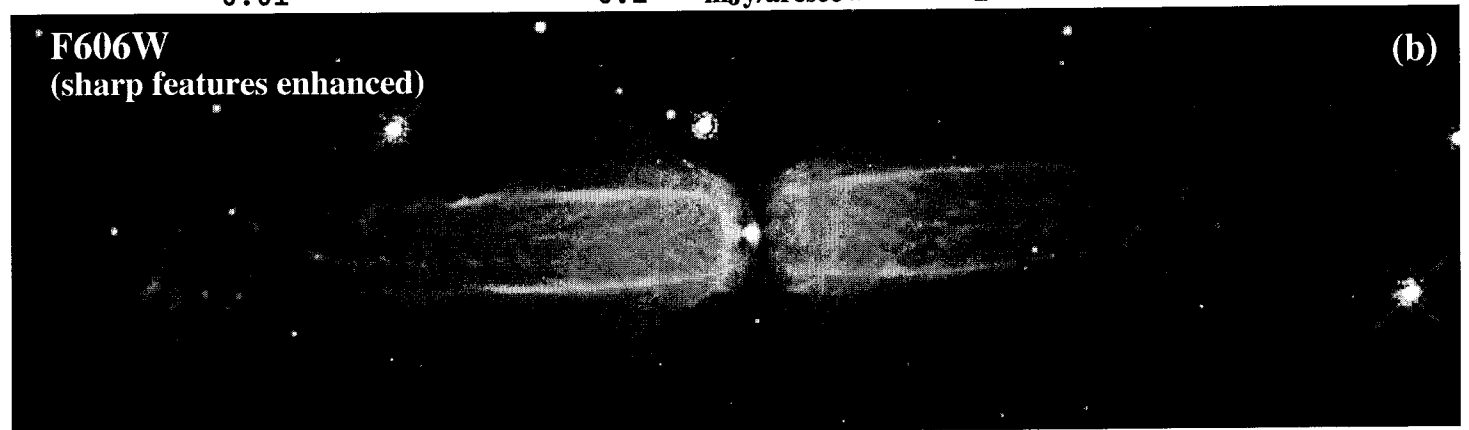
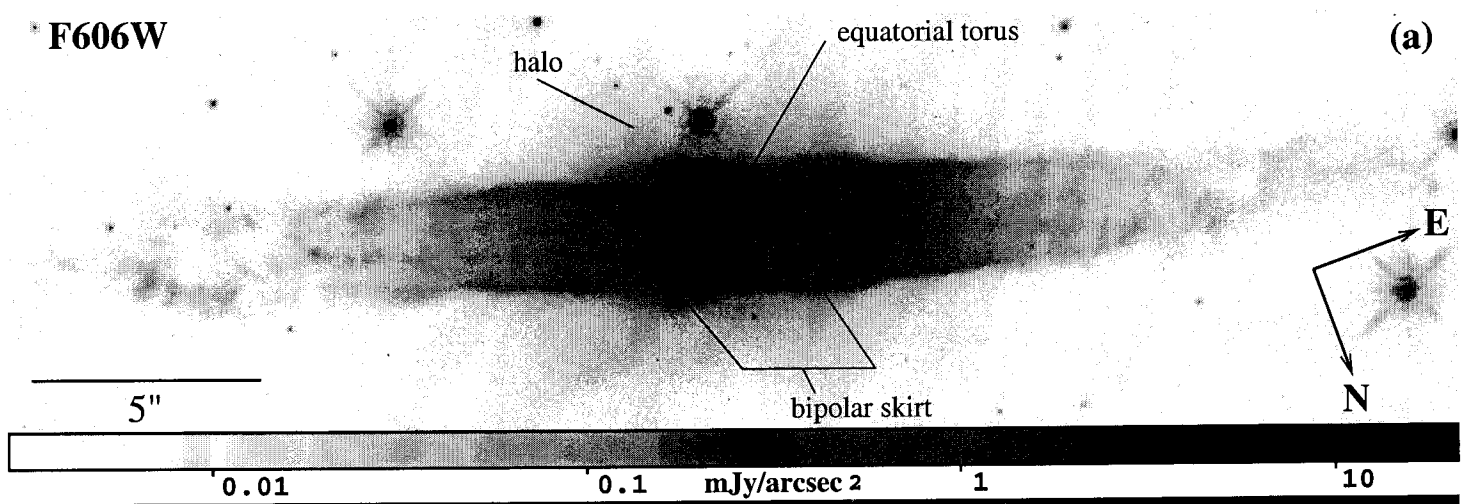


(c) F555W

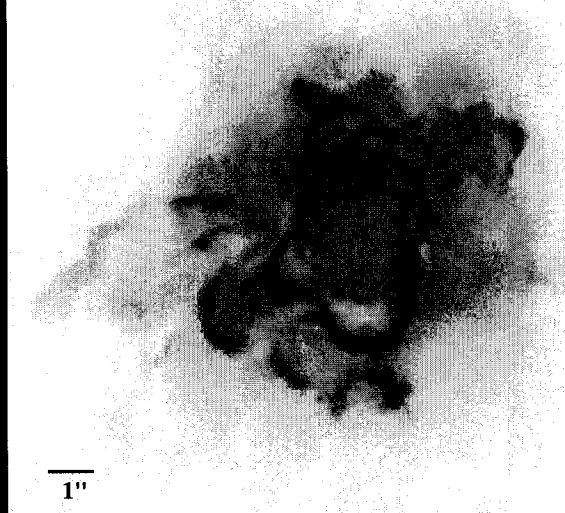


(d) F814W

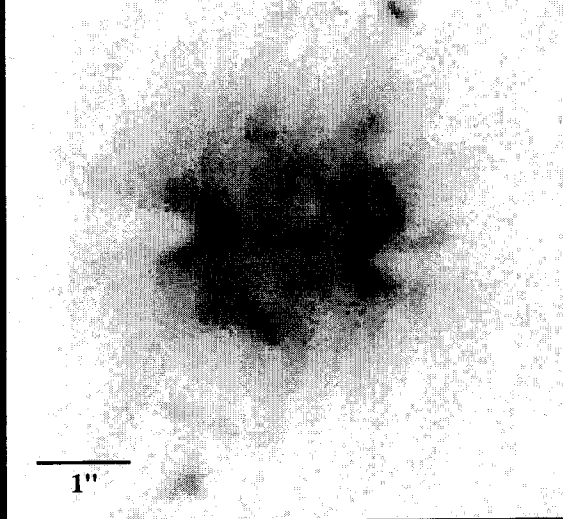




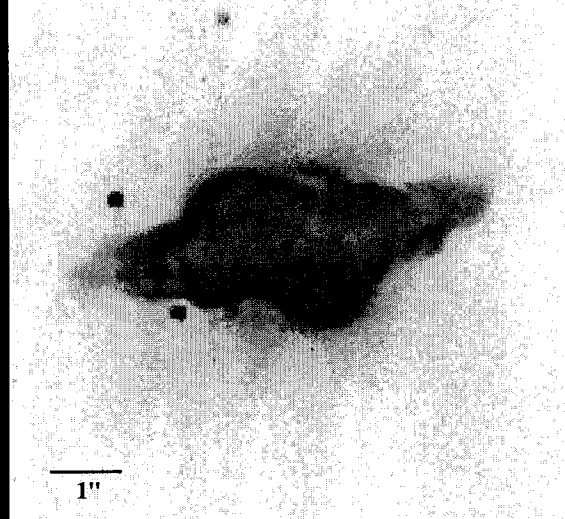
PK358-00#2 (M1-26)



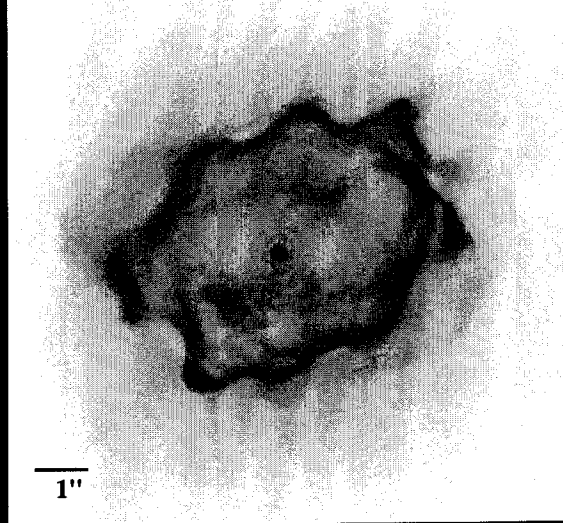
PK167-09#1 (K3-66)



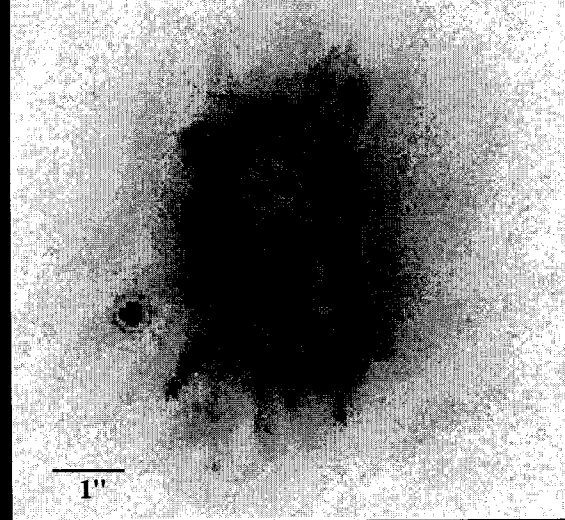
PK321+02#1 (He2-115)



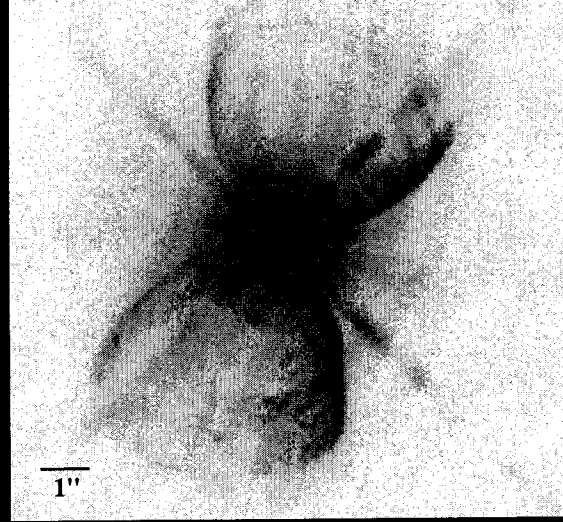
PK320-09#1 (He2-138)



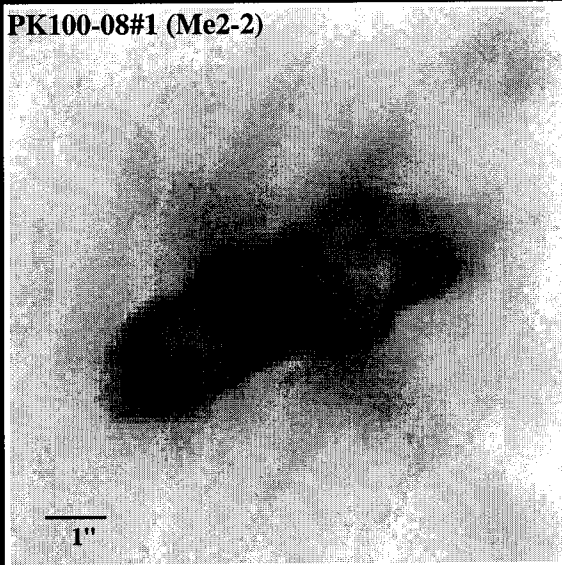
PK327-02#1 (He2-142)



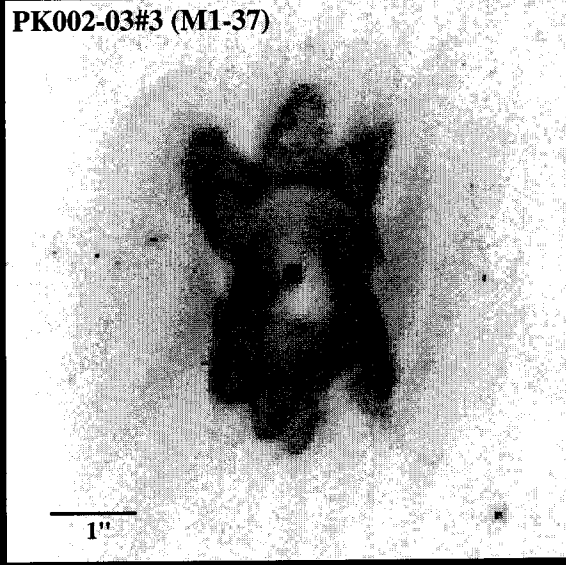
PK111-02#1 (Hb 12)



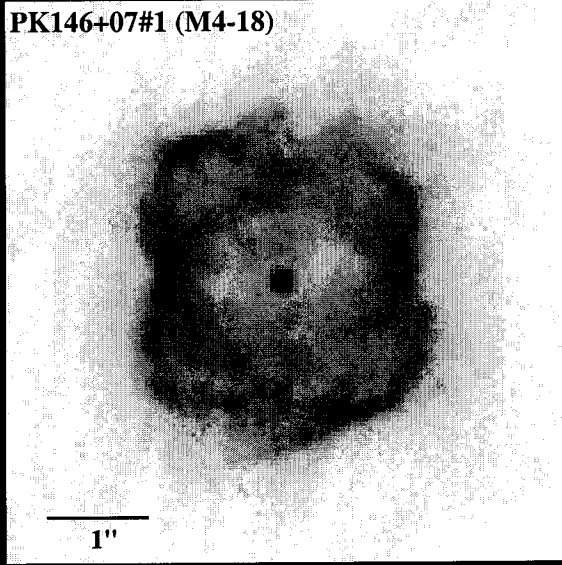
PK100-08#1 (Me2-2)



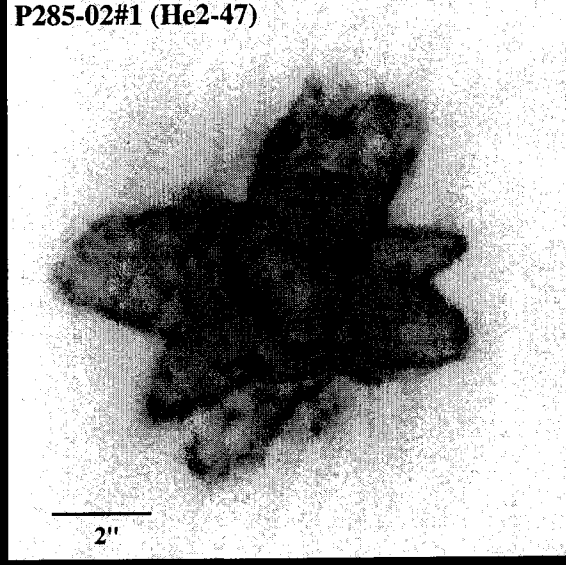
PK002-03#3 (M1-37)



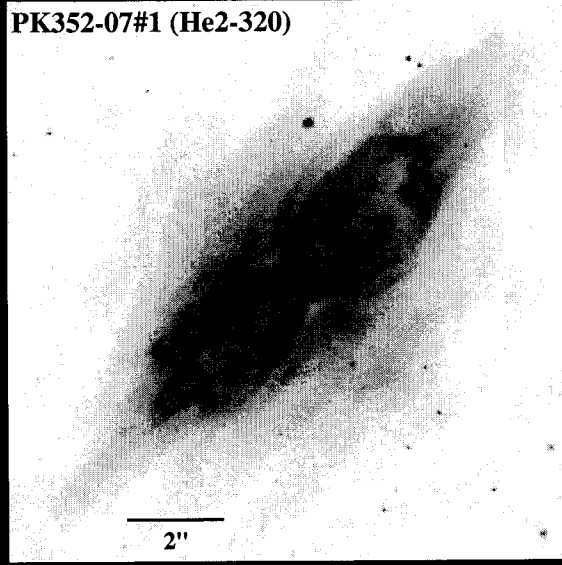
PK146+07#1 (M4-18)



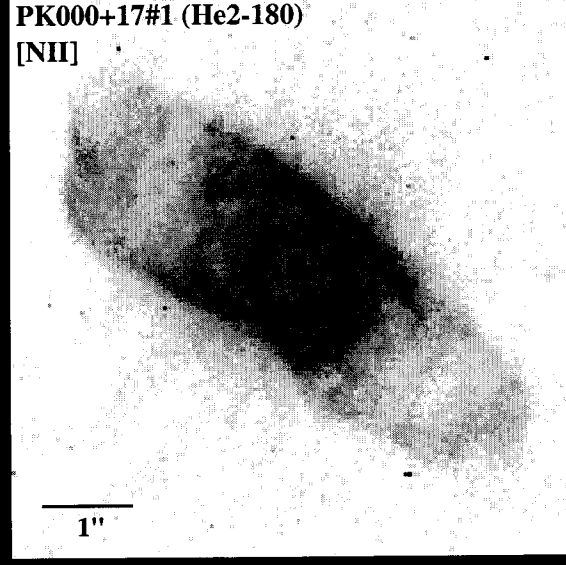
P285-02#1 (He2-47)

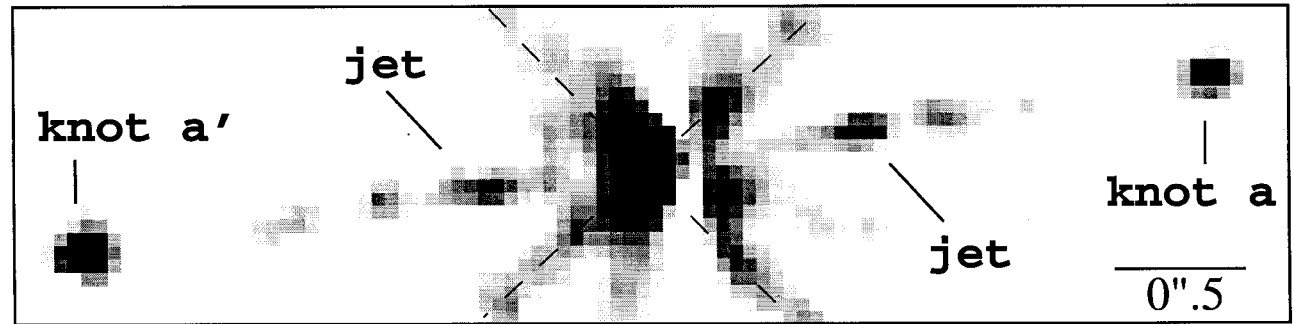
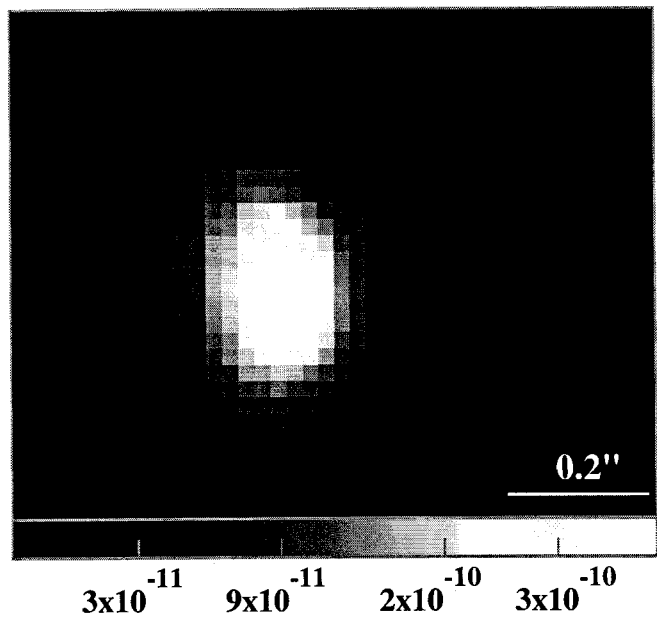
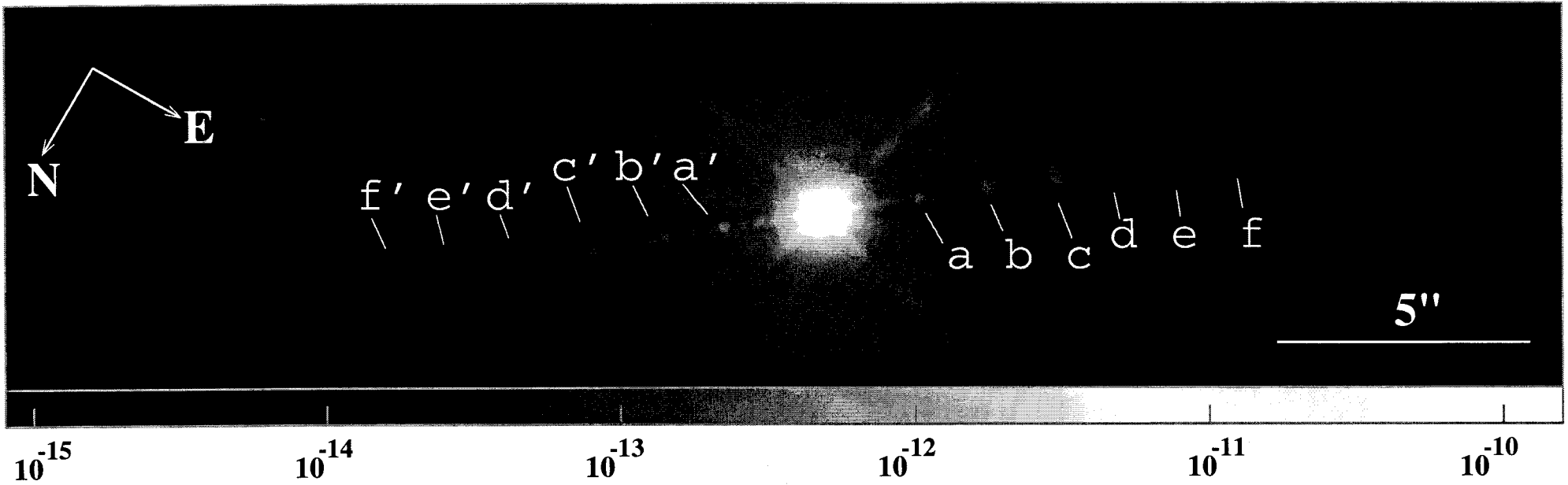


PK352-07#1 (He2-320)



PK000+17#1 (He2-180)  
[NII]





# The Bipolar Jet in the Young PN He2-90

(Sahai & Nyman 2000, ApJ Letters - in press)

# ***Results from HST: Highlights***

***(mostly from Young PNe Survey by Sahai & Trauger 1998)***

- **No Round PNe (or PPNe)**
- **Large Variety of Morphologies** - **Complexity, not Chaos**
- **Many objects are multi-lobed** - **not simply bipolar**
- **Point-Symmetry is widely manifest**
- **Inner geometric components** (e.g. rings, inner hourglasses)
- **Central star offset from centers of nebular components**
- **Faint round halos around central aspherical nebula**  
(=Remnant AGB circumstellar envelope [CSE])
- **Multiple concentric rings in extended CSE**  
- **partial spherical shells of enhanced density, spacing ~few x 100 yrs**

# ***Implications for Theoretical Models***

- **Generalised Interacting Stellar Winds Model Inadequate**
- **Primary Agent for change in symmetry of ejecta are Episodic, Wobbling, Collimated Outflows at the end of the AGB phase**
- **Outflows carve out Density Imprint inside AGB CSE (i.e. bipolar lobes in PPNe)**
- **Subsequent, fast(er) isotropic wind from central star produces full-blown aspherical PNe (details not known; wind outflow velocity is expected to increase as star shrinks)**

## ● **Origin of fast, collimated outflows**

**1) Accretion Disk in a Binary - Radiative Instability warps disk, causing it to wobble or precess**

(e.g. Morris 1987, Soker & Livio 1994, Livio & Pringle 1996)

**2) Toroidal magnetic fields in a Rotating Star - Binary companion causes precession of rotation axis**

(e.g. Chevalier & Luo 1994, Rozyczka & Franco 1996, Garcia-Segura 1997, 2000)

## ● **Origin of Internal Structures & Central Star Offsets**

**1) DENSE WAISTS -- Enhanced mass-loss from cool magnetic spots**  
(Soker 2000)

**2) CENTRAL STAR OFFSETS -- (a) Nova-like explosions**  
**(b) Stellar companion in eccentric binary orbit** (Soker et al 1998)

**3) RINGS -- Presence of Sub-Stellar or Planetary companions**  
(e.g. ST98)